Article

Response of Ecosystem Service Value to Landscape Pattern Changes under Low-Carbon Scenario: A Case Study of Fujian Coastal Areas

Guo Cai [1,2], Yuying Lin [3,4,5], Fazi Zhang [3,4], Shihe Zhang [6], Linsheng Wen [1,2] and Baoyin Li [1,2,*]

1 State Key Laboratory for Subtropical Mountain Ecology of the Ministry of Science and Technology and Fujian Province, Fujian Normal University, Fuzhou 350117, China
2 College of Geography Science and College of Carbon Neutral Future Technology, Fujian Normal University, Fuzhou 350117, China
3 School of Culture, Tourism and Public Administration, Fujian Normal University, Fuzhou 350117, China
4 The Higher Educational Key Laboratory for Smart Tourism of Fujian Province, Fuzhou 350007, China
5 Postdoctoral Research Station of Ecology, Fujian Normal University, Fuzhou 350117, China
6 College of Resources and Environment, Southwest University, Chongqing 400700, China
* Correspondence: liby@fjnu.edu.cn

Abstract: Assessing the influence of landscape pattern changes on ecosystem service value (ESV) is critical for developing land-use polies and increasing ecosystem services. The data sources include remote-sensing image data and statistical yearbooks from 2000, 2010, and 2020. This study employs the patch-generating land-use simulation model, landscape pattern index, and ecological service value estimation to analyse the changes in landscape patterns and ESV in Fujian coastal areas over the last 20 years. The landscape pattern and ESV in the future (2050) are then simulated under the low-carbon scenario (LCS), with the natural development scenario (NDS) serving as a comparison. The results show that: (1) the most noticeable changes from 2000 to 2020 are the reduced cultivated land area and the rapid expansion of construction land area. By 2050, construction land will account for 7.67% of the total land area under LCS, whereas NDS will account for 9.45%, and changes in the landscape pattern indices all indicate there will be greater variety and fragmentation of the landscape, with the NDS being more serious than the LCS; (2) From 2000–2020, the total ESV value showed a decreasing trend. In 2050, the ESV under the LCS will be 122.387 billion yuan, which is higher than the 121.434 billion yuan under the NDS. Regulating services contribute the most to the total ESV, followed by support services; and (3) In the past 20 years, except for a slight increase in water area, the ESV of other landscapes has decreased, with a net decrease of 3.134 billion yuan in total. The R^2 fitting between the area change of cultivated and construction land and the total ESV reached 0.9898 and 0.9843, respectively. The correlations between ESV and landscape indices indicate that landscape pattern changes significantly impact ESV. Simulating ESV in LCS can provide guidance for optimising landscape patterns, promoting the benign operation of the regional ecosystem, and achieving sustainable ecological development.

Keywords: ecosystem service value; scenario simulation; landscape patterns; patch-generating land-use simulation (PLUS) model; Fujian coastal areas

1. Introduction

Carbon emissions affect the ecosystem by influencing climate change, thus affecting ESV [1]. In September 2020, China put forward the goal that "carbon dioxide emissions should reach the peak by 2030 and strive to achieve carbon neutrality by 2060" at the UN General Assembly [2]. With policies such as the dual control of CO_2 emissions, major cities around the world are exploring landscape models for low-carbon scenarios [3]. To respond to the goal and mandate of carbon emission reduction, there is an urgent need to

find a reasonable balance between landscape structure and low-carbon emissions, and to increase its ecological effects accordingly [4]. Coastal areas are often the ecosystems with the relatively highest economic development but with the most intense human disturbance. This significantly alters landscape patterns which, in turn, affects the formation, distribution, and provision of ecosystem services (ESs) by changing the structure, function, and spatial patterns of ecosystems [5,6]. Therefore, assessing the response mechanisms between the value of ecosystem services and changes in landscape patterns in coastal areas based on a low-carbon perspective is important for optimising the overall benefits of ecosystem service provision and promoting coordinated socioeconomic and ecological development [7].

In 1997, Costanza proposed the following important factors to consider in ecosystem service value (ESV) assessments: first, human and other species' lives are important and their changes need to be assessed through the valuation of ESs; second, there should be greater recognition of transparent ESV in public decision-making; and third, weighing and choosing between different ESs needs to be based on ecological value valuation [8]. The valuation of ecosystem services is now increasingly used by scholars as a framework for ecosystem restoration, nature conservation, watershed management, and sustainable development. For example, Xie et al., used the Aksu River as an example to reveal the relationship of ESV with natural conditions, climate change and human activities, helping decision-makers achieve sustainable management of ecosystem service and develop land-use strategies in an arid inland–oasis river basin [9]. Gao et al. took Shijiazhuang as an example to evaluate the value of ESV under three scenarios for 2030, effectively enhancing urban ESV and safeguarding urban ecological security [10]. However, studies using ecosystem service valuation have mostly focused on watersheds and city–county areas, and lacked detailed quantifications on a macroscopic scale (e.g., provincial coastal areas). The ESV evaluation approaches are generally classified into two categories. The first category is a value evaluation based on the unit-service function, usually applied to relatively small areas. This method is complex, data-intensive, and redundant, and the determination of parameters is vulnerable to subjective factors [11]. The second technique is the equivalent-factor method, based on the unit-area value provided by Costanza et al. It is a value-transfer approach, that uses landscape as a vehicle to estimate ESV by assigning a value factor to each unit area of the ecosystem. It is more suitable for assessing ESV in large-scale areas, such as Fujian coastal areas [12–14]. However, this method needs to be based on the determined value coefficient; therefore, it is particularly critical to adapt the factor to the actual situation of the study area.

Various landscape structure simulation models have been developed to predict future changes in landscape patterns. Relative to CLUE-S, ANN [15], CA [16], and FLUS [17], the patch-generating land-use simulation (PLUS) model developed by Liang et al. has high accuracy and fast operation in simulating landscape components [18]. There has been a large body of research on the response of changing 'past-status' landscape patterns to the ESV. Some scholars have modelled changes in ESV under multiple scenarios, but fewer studies have incorporated a low-carbon scenario (LCS) in ESV as a constraint to account for future landscape pattern changes. Not only is the estimation of ESV, which is closely related to landscape patterns, highly dependent on economic drivers and development strategies, but also it is subject to considerable uncertainty. To address this issue, this study proposes a low-carbon scenario analysis to pave the way for rational decision-making in response to the development direction of future society [19].

Fujian coastal areas are situated in the lower sections of the rivers, where the topography is undulating and fragmented. There are difficulties such as environmental pollution and water and soil loss, and natural catastrophes such as typhoons and floods occur year-round. Consequently, the natural environment is quite delicate. In addition, it is located in the hub of mountain and sea areas, with a rapid rate of socio-economic development and human population growth; thus facing problems such as intensified land-use, serious land fragmentation, and reduced ESV [20,21]. This study analyses the changes in landscape patterns and ESV in Fujian coastal areas from 2000 to 2020, and uses

the PLUS model to simulate the spatiotemporal distribution of the landscape patterns in 2050 under the two scenarios of LCS and NDS, on the basis of which ESV is estimated, thus revealing the response mechanism. The objectives of this study were to: (1) explore the spatiotemporal dynamics of the landscape patterns and ESV in coastal Fujian; (2) predict landscape patterns and ESV in 2050 in response to different scenarios; and (3) reveal the response of ESV to changes in the landscape patterns. The research results provide new and actionable insights into optimising the landscape pattern and improving the ESV of Fujian coastal areas under the guidance of carbon neutrality, as well as promote the co-creation of ecological civilisation and the harmonious co-existence of human and nature.

2. Materials and Methods

2.1. Study Area

The study area is the Fujian coastal areas (between 23°73′ and 27°47′ N and 117°16′ and 120°20′ E), which are a crucial ecological transition zone and area of interlocking plant and animal distribution in China, as well as Fujian's most economically developed region. The coastal area of Fujian is adjacent to the Pearl River Delta urban agglomeration in the south, the Yangtze River Delta city cluster in the north, and the Taiwan Province across the sea [21]. It mainly includes six prefectural cities: Ningde, Fuzhou, Putian, Quanzhou, Xiamen and Zhangzhou. The total area is 5.48×10^4 km^2, accounting for 44.2% of the total area of the Fujian Province. The study area has a typical subtropical monsoon climate with average temperatures ranging from 17 °C to 22 °C and average precipitation ranging from 1200–1700 mm (Figure 1).
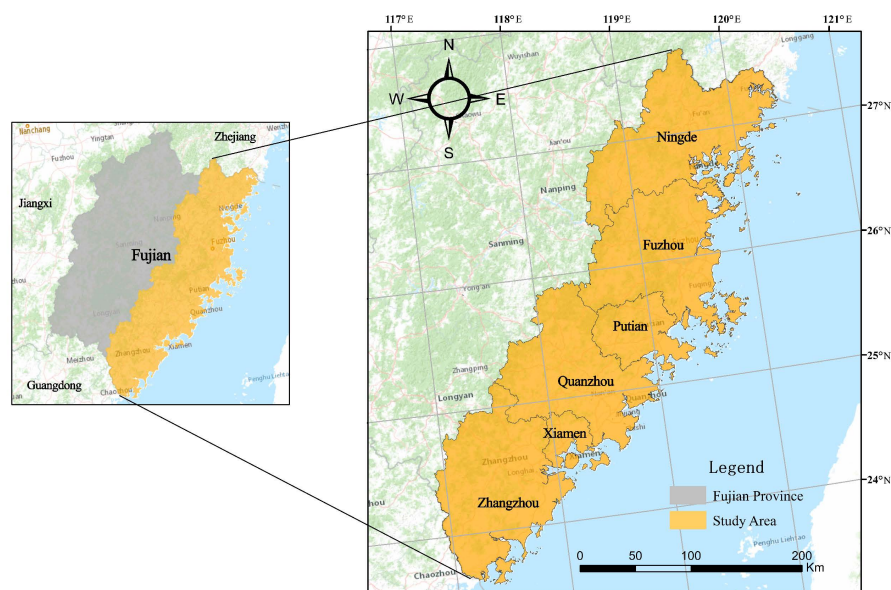
Figure 1. Geographical location and administrative division of Fujian Coastal Areas.

2.2. Data Source

This study collected three land-use maps with a spatial resolution of 30 m for 2000, 2010, and 2020. The Resource and Environmental Science Data Centre of the Chinese Academy of Sciences (http://www.resdc.cn/, accessed on 28 November 2022) classifies land-use types into six major categories including cultivated land, woodland, grassland, water, construction land and unused land. The accuracy of their maps are all over 94.3%. The drivers used in the study include natural factors, socio-economic factors and accessibility factors. The natural factors DEM was obtained from Geospatial Data Cloud, and slope and direction data were extracted from the DEM. Annual precipitation, average annual temperature and soil type data were obtained from the Resource and Environment Data Centre of the Chinese Academy of Sciences (http://www.resdc.cn/, accessed on 28 November 2022). Kilometre-grid GDP, luminous lights, population grid data and other

socio-economic factors also come from the Resource and Environmental Sciences Data Centre. Accessibility factors include the distance to different graded roads, water sources and railway stations extracted from OpenStreetMap (https://www.openstreetmap.org/, accessed on 28 November 2022). All spatial datasets were resampled to a resolution of 30 × 30 m and converted to the same projection (WGS_1984_UTM_ Zone_50N) for consistent analysis (Table A1).

2.3. Research Process and Methods

2.3.1. Research Process

The flow chart of this study mainly included four parts (Figure 2). First, the collected social and economic data was processed. Secondly, Markov chain was used to predict LUCC demand, and the PLUS model was used to distribute the demand. Thirdly, the landscape index was used to describe landscape pattern changes. Fourthly, ESV was quantified and the response of ESV to landscape pattern changes was analysed.
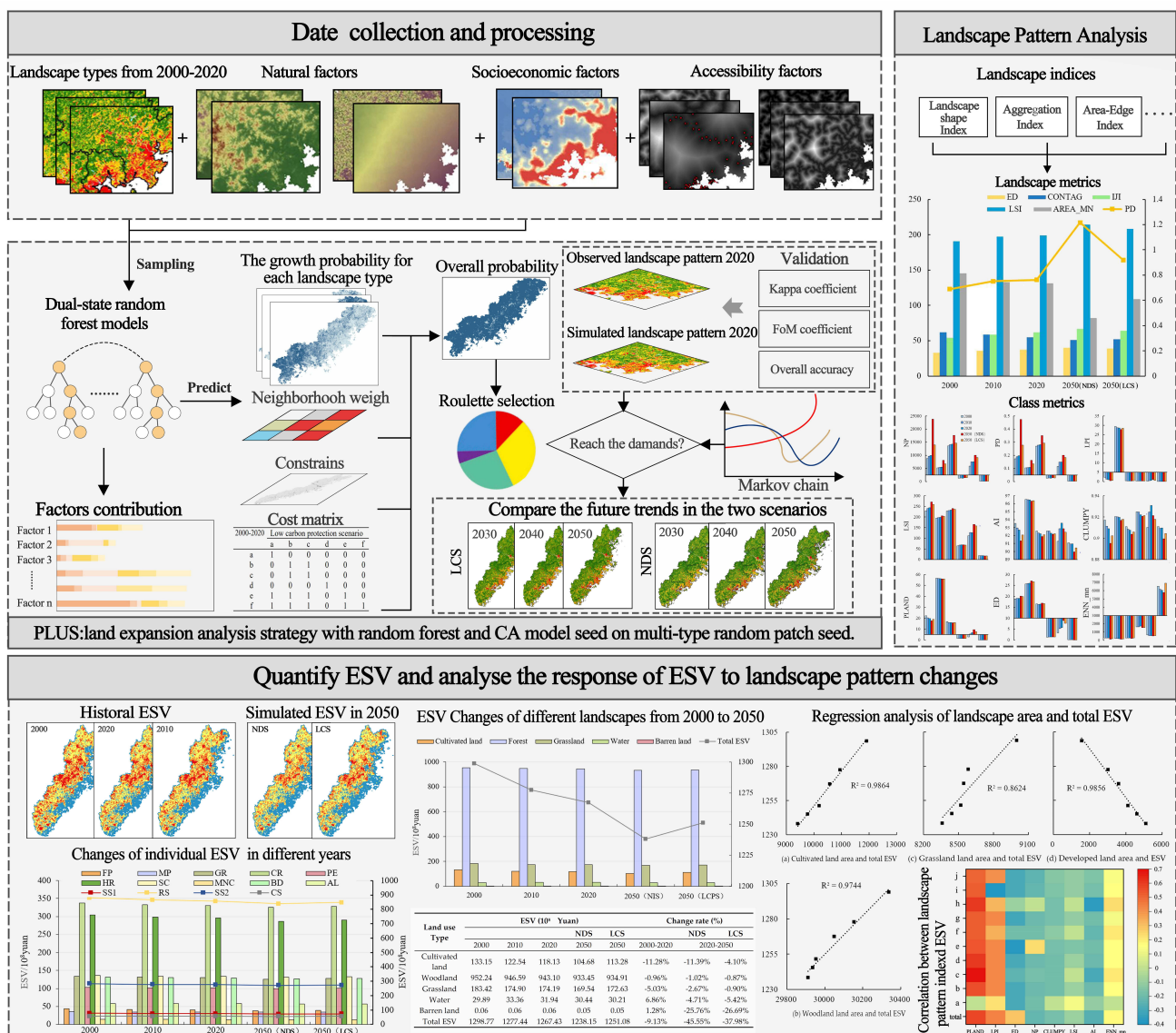
Figure 2. Research framework. PLUS: patch-generating land use simulation; ESV: ecosystem service value; LCS: low-carbon scenario; NDS: natural development scenario.

2.3.2. Landscape Types Simulation and Prediction Based on LCS

The PLUS model couples Land Expansion Analysis Strategies (LEAS), Cellular Automata (CA), Markov Chains and Random Forests [18]. First, the extension parts of various types of landscape are extracted, then the RFC is used to analyse the relationship between the extension parts and the driving variables, and to calculate the growth probability to obtain the conversion rules. Finally, the CA model is used to simulate and forecast future landscape [22].

This study chose 15 influencing factors from three aspects—natural factors, socioeconomic factors, and accessibility—and included elevation, slope, precipitation, temperature, soil type, kilometre-grid GDP, population density, night light and distance from different levels of roads. They are unified with the projection-coordinate system and spatial resolution of land cover data (Figure 3). Combined with the transfer of landscape types in the study area, the parameters were tuned several times to determine the land-use transfer-cost matrix. The probability of random patch seeding was set to 0.0001 (parameter range 0~1; a value closer to 1 means that the type of land is more likely to produce new patches). The neighbourhood-factor parameters of cultivated land, woodland, grassland, water, construction land and unused land were set to 0.11, 0.02, 0.25, 0.05, 1, 0.002 [23].
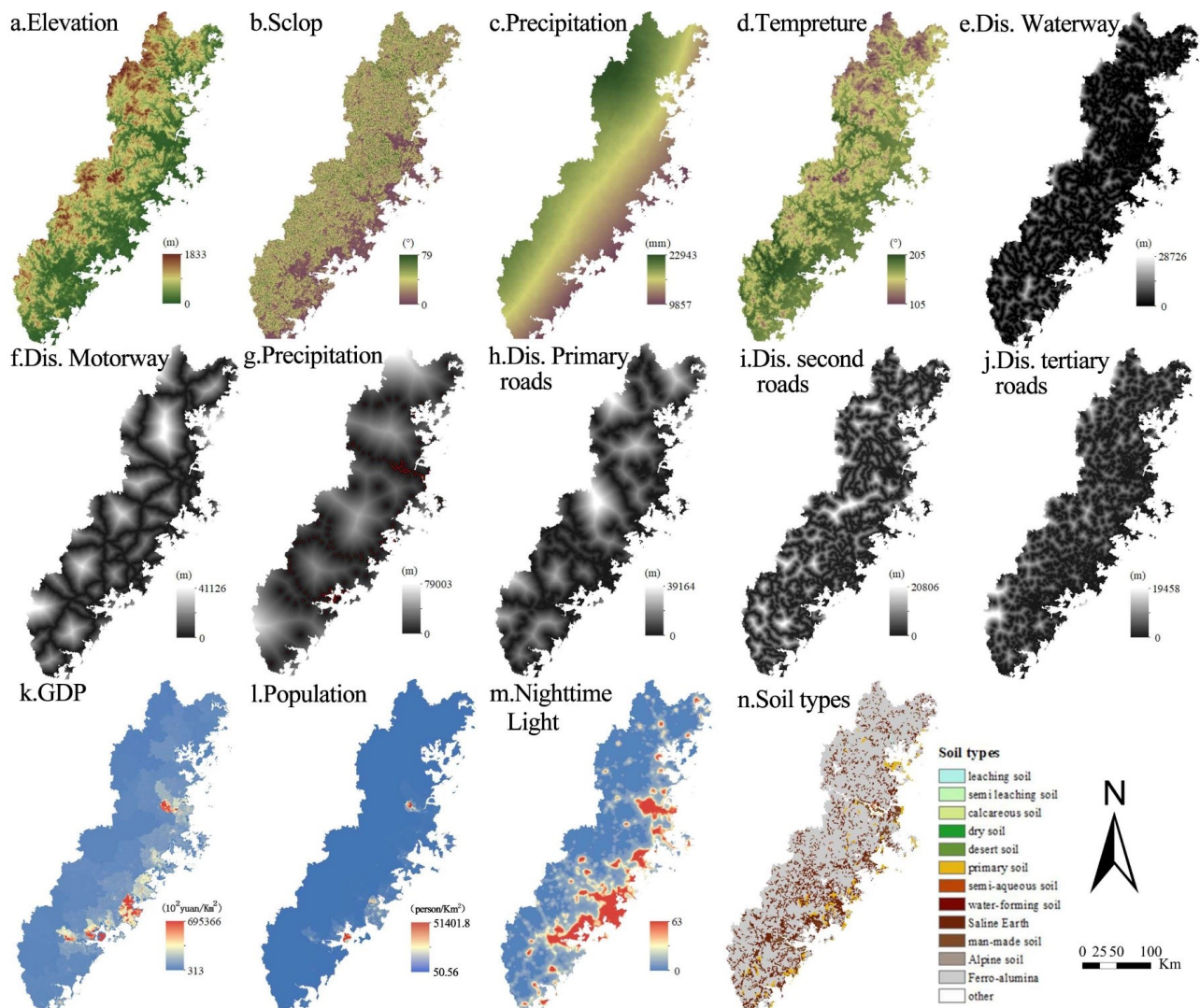

Figure 3. Drivers of LUCC conversion in Fujian coastal areas.

The accuracy of the simulation results was assessed by the Kappa coefficient and the FoM (Figure of Merit) coefficient. The Kappa coefficient is 0~1. When Kappa ≥ 0.75, the consistency between actual degree and simulation degree is high [18]. Theoretically, the FoM value ranges from 1% to 59%. The higher the value, the higher the accuracy of the simulation results. In fact, FoM is usually less than 30% [24,25].

2.3.3. Scenario Setting and Conversion-Cost Matrix

In this study, the scale of landscape development in coastal areas of the Fujian Province was constrained in accordance with the General Land Use Plan of Fujian Province (2006–2020) and the Fourteenth Five-Year Plan for National Economic and Social Development of Fujian Province and the Outline of Visionary Targets for 2035 [26]. This study establishes a LCS to predict changes in Fujian's landscape pattern in 2050, and uses the NDS as a comparison [27]. The NDS is the basis for constraining the simulation of landscape-change modelling. It directly simulates the future landscape based on the transformation of the past landscape, without the constraining influence of policy on landscape development. The LCS aims to increase carbon sink capacity and reduce carbon emissions by reducing the probability of conversion of woodland, grassland and water land into construction land, and limiting the conversion between more different landscape types, so as to add low-carbon factors into the LCS.

Under space constraints, the number of landscapes in the future is the same, but their spatial positions are different. The space constraint is mainly adjusted by changing the space-transfer matrix, and the transformation rule of the transfer matrix is whether one type of space can be converted to another type of space [28]. In the conversion-cost matrix, 0 signifies that the category cannot be transferred to another, while 1 means the reverse. In this paper, two conversion-cost matrices are set for different scenarios (Table A2).

2.3.4. Index-Selected Landscape Patterns

Landscape indices are extremely condensed information about landscape patterns that reflect their structural composition and spatial configuration. Because some landscape indices are redundant, we chose typical indices to reflect the landscape patterns based on actual situation and research demands [29]. Twelve landscape indices were selected on the two scales of patch type and landscape level. These included the number of patches (NP); patch density (PD) and average patch area (AREA_mn) that can reflect the density and difference; the percentage of patch area (PLAND) and the largest patch (LPI) that reflect the change of area size; the average European nearest neighbour distance (ENN_mn) that reflects the proximity of patches; Edge density (ED) and landscape shape (LSI), reflecting changes in landscape shape; as well as conglomeration index (CLUMPY), aggregation index (AI), dispersion in juxtaposition index (IJI) and contagion index (CONTAG), reflecting aggregation and dispersion (Table A3) [30–32]. All indices were used with Fragstats 4.2.1 to quantify the spatial and temporal characteristics of landscape change [33].

2.3.5. Estimation of ESV and Correction of Coefficients

Xie et al. set the food production function of farmland to 1, which represents the economic value of natural food production per unit area of farmland per year on average throughout the nation [34,35]. In this study, the economic value of food production per unit area was revised to match the ecosystem assessment of the Fujian coastal areas, where the ESV for construction land was defined as 0 (Table A4) [36,37].

Considering the land-use change under the regional background, the sown area, yield, and average price of three major crops (rice, sweet potato and soybean) in Fujian coastal areas from 2000 to 2020 were taken as the basic data. The economic value of food crops per unit area of ecosystem in Fujian coastal areas was calculated as 1817.8 yuan/hm^2 according to Equation (1). The estimation formula is:

$$Ea = 1/7 \sum_{i=1}^{m} \frac{o_i p_i q_i}{M} \quad m = (1,2,3) \tag{1}$$

where *Ea* is the economic value of the ecological service equivalent factor per unit area of farmland in Fujian coastal areas, and o_i is the area of the *i*th food crop (hm^2); p_i is the yield of the *i*th food crop (kg/hm^2); q_i is the average price of food crop *i* (yuan/kg); and *M* is the total area of the three food crops. The unit area ESV of Fujian coastal landscape types was determined by using the ecosystem service coefficient and land-use area (Table 1).

Table 1. Coefficient tables of ESV in the study area (Unit: Chinese yuan (RMB)/ha).

Ecosystem Service	Class	Cultivated Land	Woodland	Grassland	Water	Unused Land
Supply Service	FP	2472	424	424	464	18
	RM	164	976	624	454	55
Regulation Service	GR	2018	3199	2193	1745	200
	CR	1036	9574	5799	3272	182
	PE	309	2848	1915	3363	564
	HR	4944	6926	4248	22050	382
Support Service	SFM	18	3896	2672	2118	236
	MNC	345	297	206	164	18
	BP	382	3551	2430	7171	218
Cultural Service	AL	164	1557	1073	4308	91

According to Table 1, the total ESV, the ESV of each landscape land type and the individual service function values for the Fujian coastal areas from 2000 to 2050 were obtained respectively and calculated as follows:

$$ESV = \sum A_i \times VC_i \tag{2}$$

$$ESV = \sum A_{if} \times VC_{if} \tag{3}$$

where *ESV* represents the total regional ecosystem service value ($); A_i represents the area of the *i*th landscape type (hm^2); VC_i represents the value coefficient for landscape type *i* [($hm^{-2} a^{-1})]; ESV$_f$ represents the value of a single ecosystem service ($); and VC_{if} represents the value coefficient of a single service [($hm^{-2} a^{-1})].

2.3.6. ESV and Landscape Patterns Index Correlation Test

The study used SPSS.21 software to calculate Pearson correlation coefficients between landscape indices and the ESV at a grid cell of 3 km × 3 km, flagging correlations above the 0.05 level of significance to reflect the influence of landscape patterns indices on the ESV.
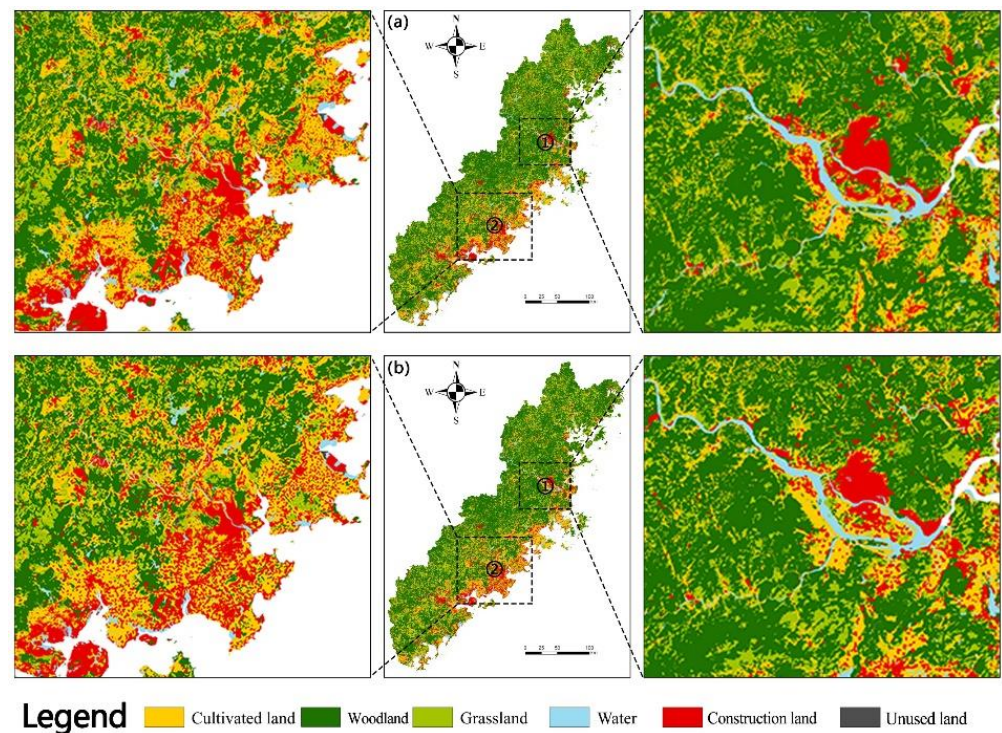
3. Results

3.1. Spatiotemporal Characteristics of Landscape Transition and Landscape Pattern Evolution under LCS Simulation

3.1.1. Spatiotemporal Characteristics of Landscape Transition

Based on the pattern of landscape type changes in Fujian's coastal region from 2000 to 2010, the 2020 landscape distribution (Figure 4b) was simulated and compared with the actual landscape distribution (Figure 4a). The simulation results are generally in good agreement with the observed landscape distributions. The accuracy of its precision was verified by the Kappa and FoM coefficients, which had a Kappa value of 0.889 and FoM value of 0.141, respectively, making the PLUS model suitable for predicting future landscape changes in the coastal region of Fujian.

The landscape types were converted from 2000 to 2020. Cultivated land and woodland had the highest turnover, with turnover areas of 1522 km^2 and 739 km^2, respectively. The main direction of turnover was construction land, with turnover areas of 1361 km^2 and 520 km^2. In addition to cultivated land and woodland, grassland and water bodies were also the main contributors to the increase in construction land area, and the transferred areas were 229 km^2 and 199 km^2, respectively (Table A5).

Figure 4. Observed and simulated results of landscape types: (**a**) observed landscape types of 2020; (**b**) simulated landscape types of 2020.

Based on the current landscape distribution between 2000 and 2020, the distribution of landscape types between 2030 and 2050 was predicted under the NDS and the LCS (Figure 5). The results showed that the historical and simulated landscapes in the Fujian coastal area had similar spatial distribution. In 2020, the woodlands accounted for 56.14% of the total area, mainly distributed in the west and north of the study area. The second largest landscape type was cultivated land, with a percentage area of 19.73% in 2020, mainly located in Zhangzhou, Quanzhou, and Ningde. Grassland had an area of 15.97% in 2020, and was located primarily in Ningde, Zhangzhou, and Quanzhou. Construction land was concentrated in the Min Delta, with 69% of the total construction land in Quanzhou, Xiamen, and Zhangzhou and 18% of the total construction land in Fuzhou. The water body in Fuzhou accounted for 34.48% of the total water body area, followed by Zhangzhou and Ningde, which together accounted for 43.86%. Under the two scenarios of LCS and NDS, construction land will expand by 2030, 2040, and 2050. The proportion of construction land in the LCS ranged from 5.58%, 6.62% to 7.67%, whereas that in the NDS ranged from 7.65%, 8.57% to 9.45%. It can be seen that the expansion of construction land in the NDS is more extensive than that in the LCS. Areas with greater construction land expansion per unit area were mainly in Xiamen and Quanzhou. In contrast, the proportion of cultivated land between 2030 and 2050 declined in both scenarios, with the NDS declining more than the LCS. The rest of the land-use types did not change significantly.
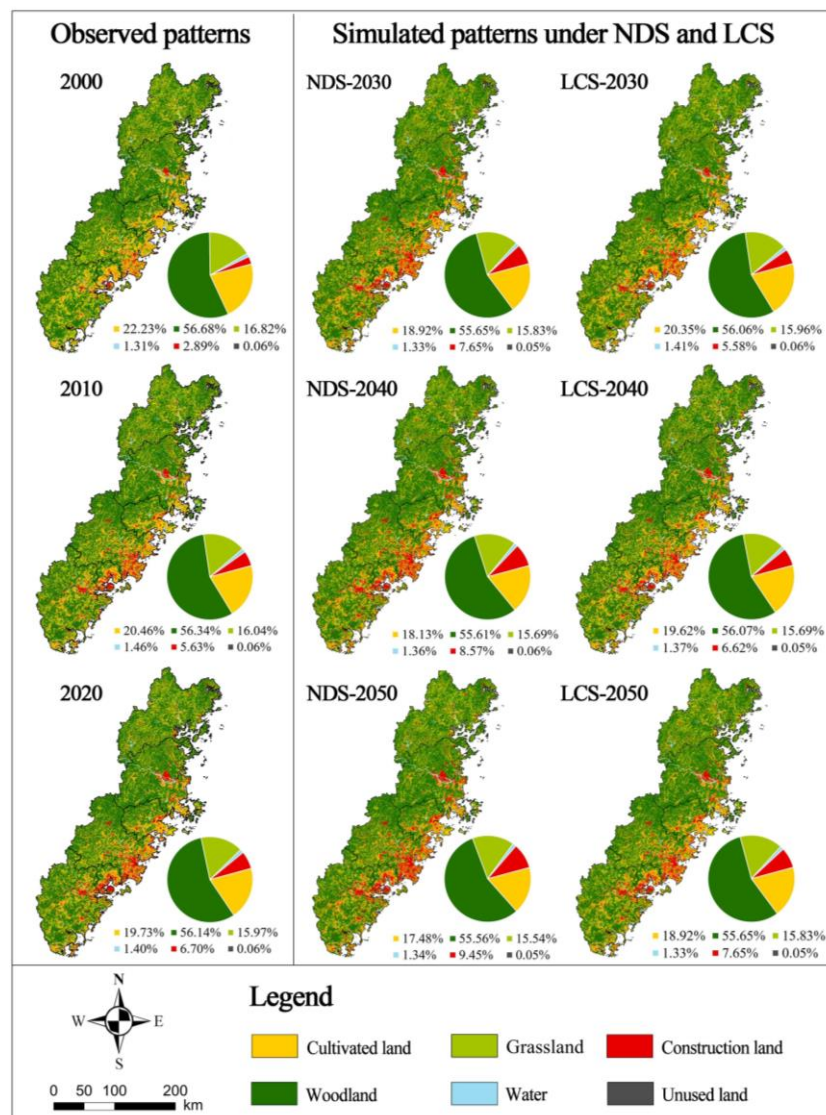
Figure 5. Spatial distribution of landscape types in Fujian coastal area from 2000 to 2050.

3.1.2. Spatiotemporal Characteristics of Landscape Pattern Changes

The ED, LSI and PD indices at the landscape level increased over the research period, showing that landscape fragmentation increased, and the shape tended to become more complicated. The CONTAG index, which reflects the spreading trend, and AREA_mn, which reflects the average size of patches, decreased, indicating that the continuity between landscape types became lower and gradually fragmented. The IJI demonstrated the degree of separation between landscapes, with larger values indicating more adjacent landscape types. From 2000 to 2020, the IJI increased from approximately 54.12 to 62.17, and the IJI index will reach 66.63 in 2050 under NDS, which further indicates that the landscape fragmentation is increasing; the PAFRAC index and SHAPE_mn index remain at approximately 1.4 and 1.9, respectively, with no apparent fluctuation trend, indicating that the overall shape of the landscape is relatively simple between 2000 and 2020. In 2050, the PAFRAC and SHAPE_mn indices remain stable at approximately 1.3 and 1.9 under LCS, respectively, whereas these fall to 1.29 and 1.21 under the NDS (Figure 6).
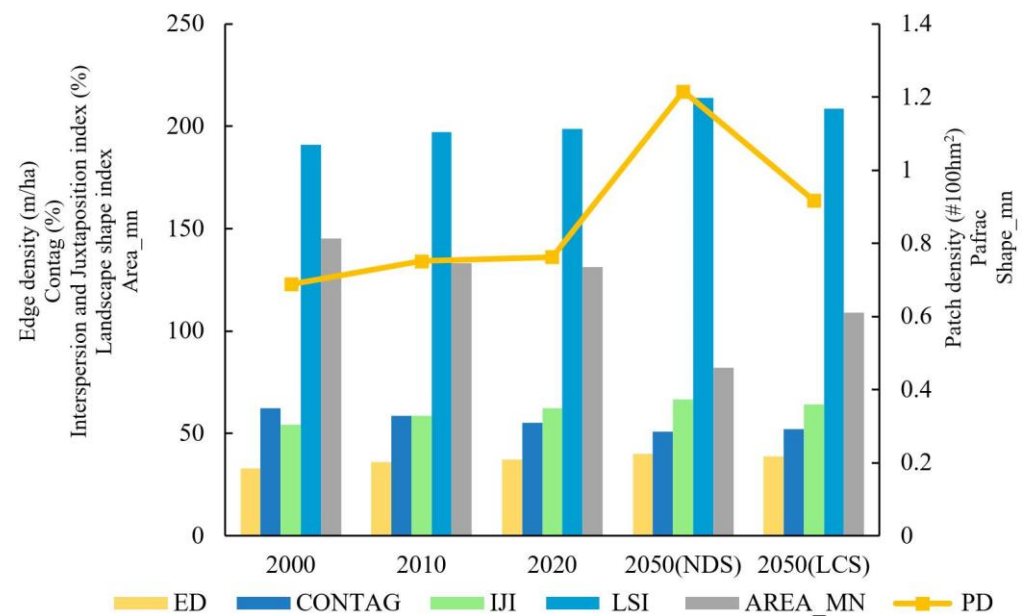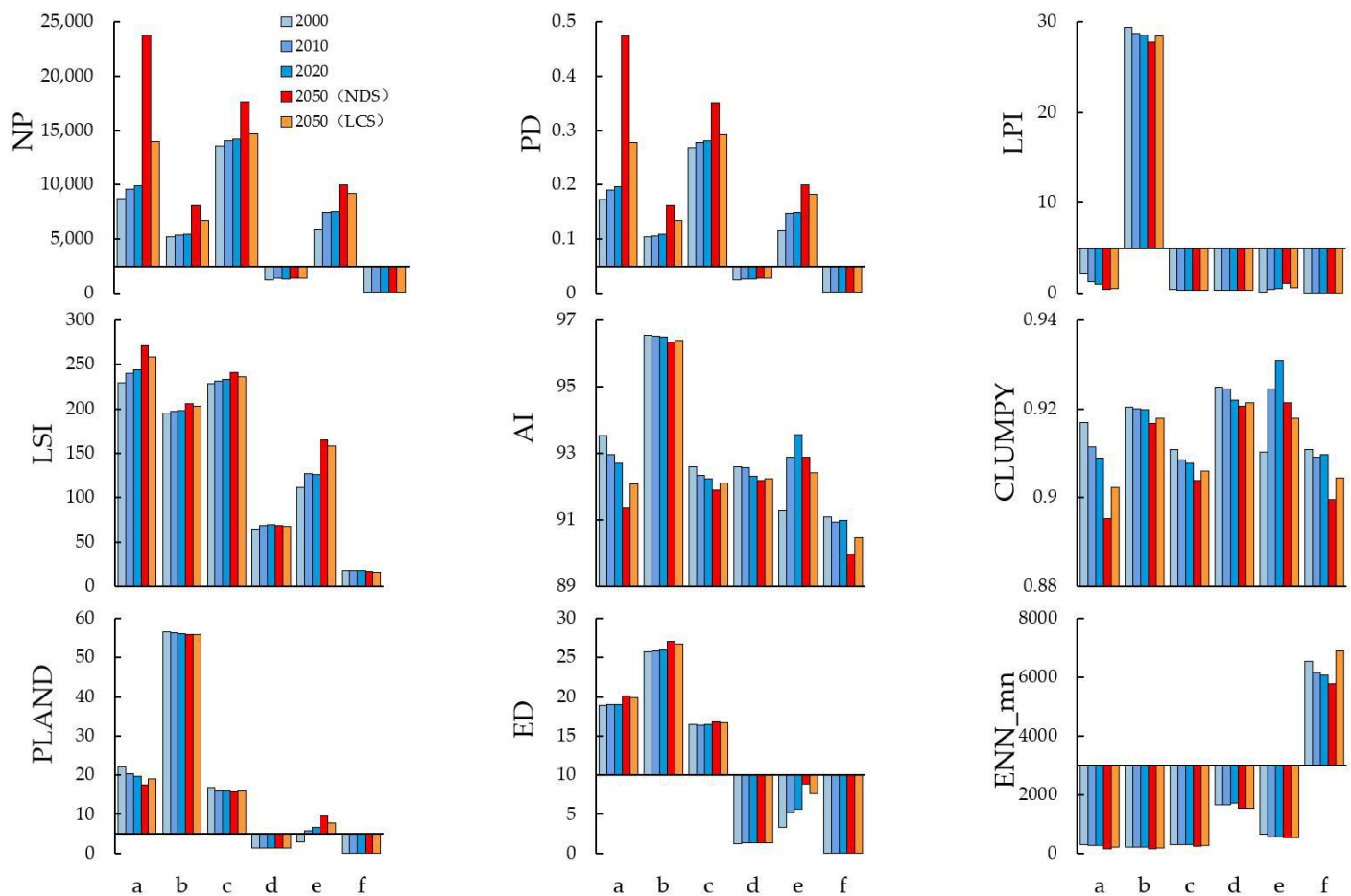
Figure 6. Landscape patterns index at the landscape level in Fujian coastal areas from 2000 to 2050.

At the landscape-type level, the LPI and PLAND indices for woodland were consistently significantly higher than for other landscape types, verifying the dominance of woodland landscape types, as represented in the Figure 7. Except for construction land, the LPI and PLAND indices of other landscape types decreased yearly. It is worth noting that under the LCS, the decreasing trend of the indices is significantly convergent compared with that under the NDS. The increasing trend of the PD and NP indices for each landscape type indicated an increase in fragmentation and complexity of shape, with fragmentation more pronounced in the NDS, most notably in cultivated land and grassland. ED is the edge density; the larger its value, the higher is the landscape fragmentation. Woodland and cultivated land have a larger ED, but the rising trend is not apparent across the years; the ED of construction land is lower, but the increasing trend is more obvious. At the same time, both the CLUMPY and AI indices continued to decrease, indicating that their landscape connectivity was further weakened and the aggregation of patches became weaker. The ENN_mn index for unused land is significantly higher than that for other landscapes, indicating that unused land is further apart from each other, whereas the values of this index for other types of land are always low and weakly changing, indicating that the rest of the landscape is consistently more densely distributed. A decreasing trend in ENN_mn is also evident for unused land; however, in the LCS, an increase occurs in 2050.

3.2. Spatiotemporal Characteristics of ESV under LCS Simulation

3.2.1. Spatiotemporal Distribution of ESV

In this paper, a 3 km × 3 km grid is used to express the spatial variation in the total ESV in Fujian coastal areas from 2000 to 2050, and the values per unit grid are classified into I (0–1.5×10^7 yuan), II (1.5–2.0×10^7 yuan), III (2.0–2.5×10^7 yuan), IV (2.5–2.8×10^7 yuan), and V ($>2.8 \times 10^7$ yuan) categories (Figure 8).

Figure 7. Landscape patterns index at landscape type level in Fujian coastal areas from 2000 to 2050. Abbreviations: a (cultivated land), b (woodland), c (grassland), d (water), e (construction land), f (unused land).

The ESV in the Fujian coastal area showed a decreasing trend in space. The area with a low ESV was gradually expanded, and the area with a high ESV value gradually reduced, especially in the midwest of Fuzhou City, west of Quanzhou City and the south of Zhangzhou City. This was mainly because of the gradual increase in landscape segmentation caused by the accelerated urbanisation process, which reduced the cultivated land landscape area and expanded the landscape fragmentation process from the coastal areas to the central part of the Fujian Province, thus leading to spatial changes in the ESV in the study area [38]. According to statistics, the ESV in 2000, 2010, and 2020 was 129.877 billion yuan, 127.744 billion yuan, and 126.743 billion yuan, respectively, showing an all-time decreasing trend. By 2050, the ESV under the NDS will be 123.815 billion yuan, whereas that under the LCS will be 125.109 billion yuan, an increase of 1.294 billion yuan, indicating that the optimised LUCC structure is consistent with the LCS objective.
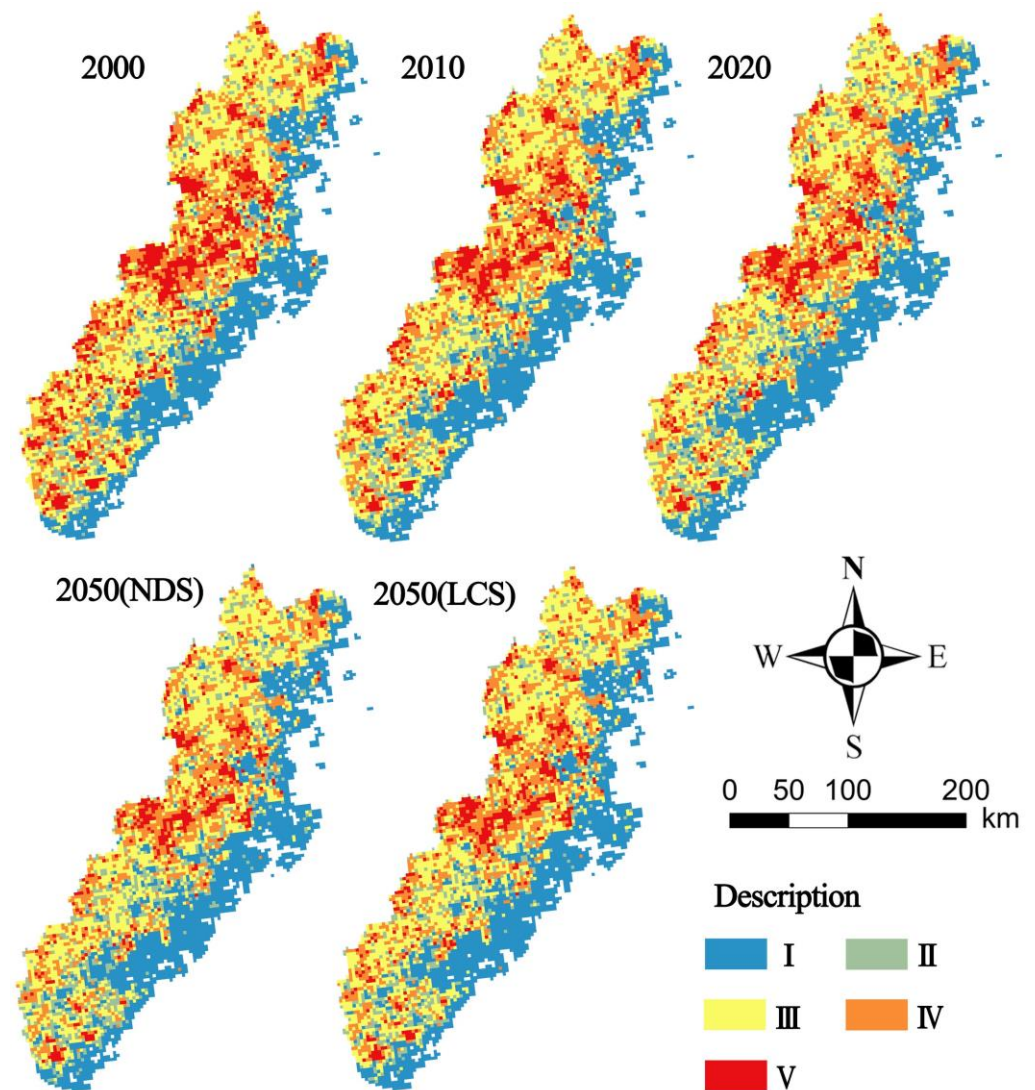
Figure 8. Spatial distribution map of total ESV variation in coastal areas of Fujian from 2000 to 2050. NDS: natural development scenario; LCS: low-carbon scenario.

3.2.2. Change Characteristics of Individual ESVs

The first-level service function of a single ecosystem regulates services that contribute the most to the ESV in coastal areas of Fujian, with a total ESV exceeding 83 billion in the past 50 years, accounting for approximately 67% of the total contribution. Support services are second only to regulating services, with a total value of over 27 billion and a contribution of over 20%. In terms of individual secondary ESs, climate, hydrological, soil conservation, biodiversity, and gas regulation are the most important ESs in coastal Fujian. From 2000 to 2050, the ESV of climate regulation was more than 32.5 billion yuan, and the ESV of hydrological regulation was more than 28.5 billion yuan, contributing more than 20% to the ESV of each period. The ESV of soil conservation, biodiversity, and gas regulation was more than 12.5 billion yuan, contributing more than 10% of the ESV in each period. The above five categories contributed to more than 80% of the ESV (Figure 9).
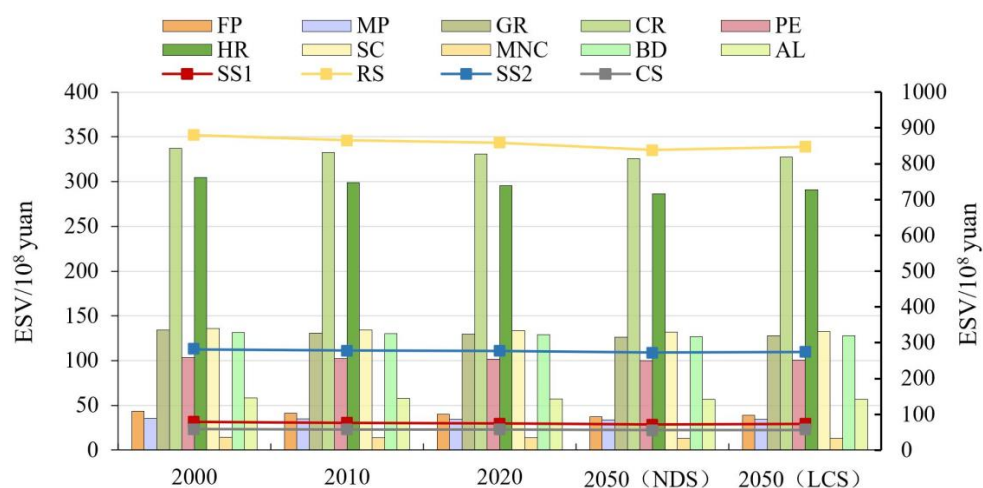
Figure 9. Changes in the individual ecosystem service value (ESV) in Fujian coastal areas from 2000 to 2050. Food production (FP), material production (MP), gas regulation (GR), climate regulation (CR), purified environment (PE), hydrological regulation (HR), soil conservation (SC), maintain nutrient cycle (MNC), biodiversity (BD), aesthetic landscape (AL), supply services (SS$_1$), regulating services (RS), support services (SS$_2$), cultural services (CS).

The overall ESV decreased from 2000 to 2020, with a change rate of 28.6%. From 2020 to 2050, the overall ESV also dropped, with a change rate under NDS of 27.3%, whereas it was 14.11% under LCS. Among the individual ESV, the decline rate of food production was the largest, reaching 7.78% from 2000 to 2020, which is related to the loss of cultivated land in Fujian coastal areas. The rate of change of ESV in food production will still rank first by 2050. Under the NDS, the decline rate of food production reached 7.51%, and under the LCS, the decrease rate was 2.88%, indicating that LCS can reduce the serious situation of farmland loss (Table 2).

Table 2. Changes in ESV in the study area from 2000 to 2050 ($\times 10^8$ yuan/hm^2).

Ecosystem Service	Class	ESV Change Rate (%)		
			NDS	LCS
		2000–2020	2020–2050	
Supply services	FP	7.78	7.52	2.89
	MP	2.03	1.79	1.07
	GR	3.21	2.90	1.42
Regulating services	CR	1.86	1.60	1.01
	PE	1.78	1.68	1.08
	HR	2.95	3.14	1.65
	SC	1.57	1.35	0.93
Support services	MNC	4.21	3.81	1.69
	BD	1.65	1.73	1.15
Cultural services	AL	1.54	1.76	1.20
Total ESV		28.6	27.3	14.11

3.3. Response of ESV to Landscape Pattern Changes

Landscape patterns caused changes in the ESV in the Fujian coastal areas. The areas with medium–high ESV values were mainly distributed in dense woodland and grassland areas with relatively complete natural ecosystems, whereas the areas with low ESV values were primarily distributed in areas with high population density, apparent urban expansion, and serious loss of cultivated land. From 2000 to 2020, the main landscape change pattern was the mutual shift between cultivated, woodland, and grassland (Table A5). The area of construction land increased, whereas the area of other land-uses, such as cultivated

land and grassland, decreased. Accelerated urbanisation has led to the rapid expansion of construction land at the expense of large areas of cultivated land, which has reduced the ESV of cultivated land in coastal Fujian by RMB 1.502 billion between 2000 and 2020 [39].

Predicting the change in ESV under the NDS and LCS provides a basis for realising the dual control goal of CO_2 emissions in China and sustainable land-use decisions [40,41]. The ESV in coastal areas of Fujian increased first and then decreased, with a net increase of 205 million yuan (6.86%), whereas the rest of the landscape types decreased, with a net decrease of 3.134 billion RMB in the total ESV. By 2050, the ESV of all landscapes will show a downward trend, but the decline value in the next 30 years will be slightly lower than that in the previous 20 years. The decline rate of cultivated land in 2050 under LCS is 4.10%. Compared with the decline rate of cultivated land in the NDS of 11.39%, the decline in ESV was greatly mitigated (Figure 10) (Table 3).
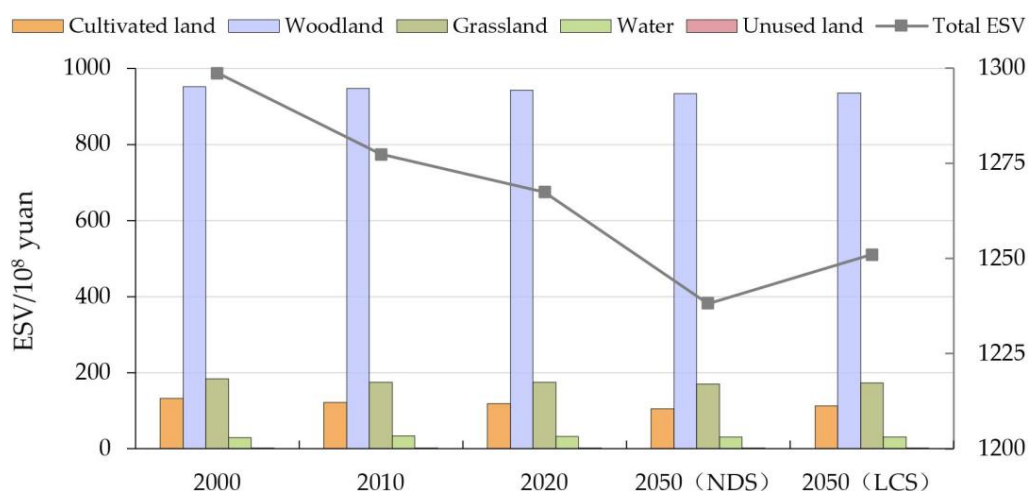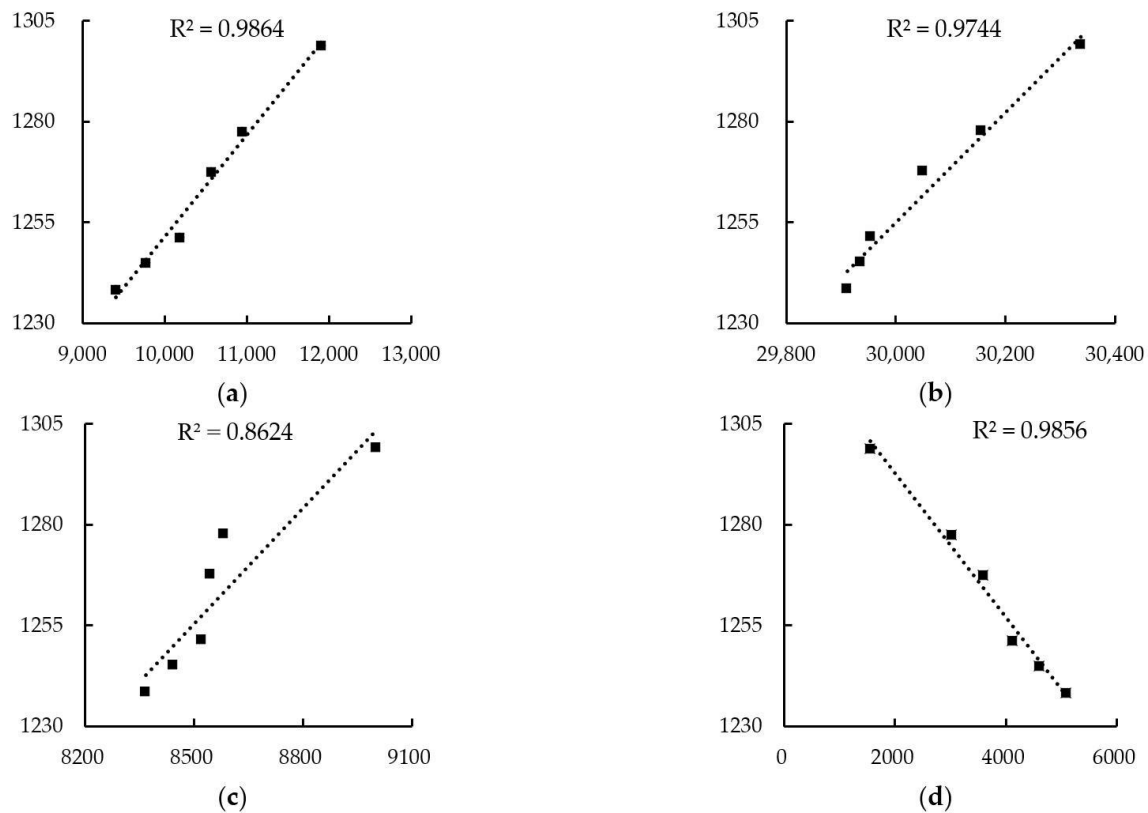

Figure 10. Changes in ecosystem service value (ESV) of different landscapes from 2000 to 2050.

Table 3. Changes in ESV of different landscape types from 2000 to 2050.

| Landscape Type	ESV (10^8 Yuan)					Change Rate (%)		
				NDS	LCS		NDS	LCS
	2000	2010	2020	2050	2050	2000–2020	2020–2050	
Cultivated land	133.15	122.54	118.13	104.68	113.28	11.28	11.39	4.10
Woodland	952.24	946.59	943.10	933.45	934.91	0.96	1.02	0.87
Grassland	183.42	174.90	174.19	169.54	172.63	5.03	2.67	0.90
Water	29.89	33.36	31.94	30.44	30.21	6.86	4.71	5.42
Barren land	0.06	0.06	0.06	0.05	0.05	1.28	25.76	26.69
Total ESV	1298.77	1277.44	1267.43	1238.15	1251.08	9.13	45.55	37.98

The area of the six landscape types was correlated with the total ESV in the NDS from 2000 to 2050, and a simple regression analysis was conducted between the areas of the four landscape types that are strongly associated with the total ESV: cultivated land, woodland, grassland and construction land (Figure 11). The changes in cultivated and construction land areas fit the total ESV best, with R^2 as high as 0.9864 and 0.9856, respectively, explaining the changes in ESV well. Woodland and grassland also fit better, with R^2 values of 0.974 and 0.862, respectively, complementing the results of the correlation analysis. In contrast, unused land and water correlated less well with the total ESV. The results show that an increase in the area of construction land caused a decrease in the total ESV, and an increase in the area of other types of landscape caused an increase in the total ESV. From 2000 to 2050, the area of cultivated land, woodland, and grassland under the

NDS decreased by 1204 km^2, 310 km^2, and 230 km^2, respectively, and their ESV volume decreased by 2.847 billion yuan, 1.879 billion yuan, and 1.388 billion yuan, respectively.

Figure 11. Regression analysis of the change in landscape area of cultivated, woodland, grassland and construction land and total ecosystem service value (ESV). (**a**) Cultivated land area and total ESV; (**b**) Woodland land area and total ESV; (**c**) Grassland land area and total ESV; (**d**) Construction land area and ESV.

The total ESV was significantly positively correlated with PLAND, LPI, and AI indices, and negatively correlated with ED and NP, but not significantly correlated with CLUMPY, LSI, and ENN_mn indices. This shows that the greater the number and complexity of the shape of the landscape, the lower the ecological service value, whereas the concentration of patches and the increase in landscape dominance were conducive to the enhancement of ESV. The correlation between the landscape index and individual ESV was broadly similar to that between the landscape index and the total ESV. In addition, the ESV of food production had a strong negative correlation with ED and NP. CLUMPY had a strong negative correlation with the ESV of raw material production, gas regulation, and climate regulation. ENN_mn was only strongly positively correlated with the ESV of gas regulation, hydrological regulation, and nutrient cycling. NP was weakly correlated with the ESV of soil conservation but not the ESV of gas regulation. The ESV of food production, biodiversity, and aesthetic landscapes were weakly correlated with AI. The ESV of gas regulation, hydrological regulation, and nutrient cycling were weakly correlated with ED (Figure 12).
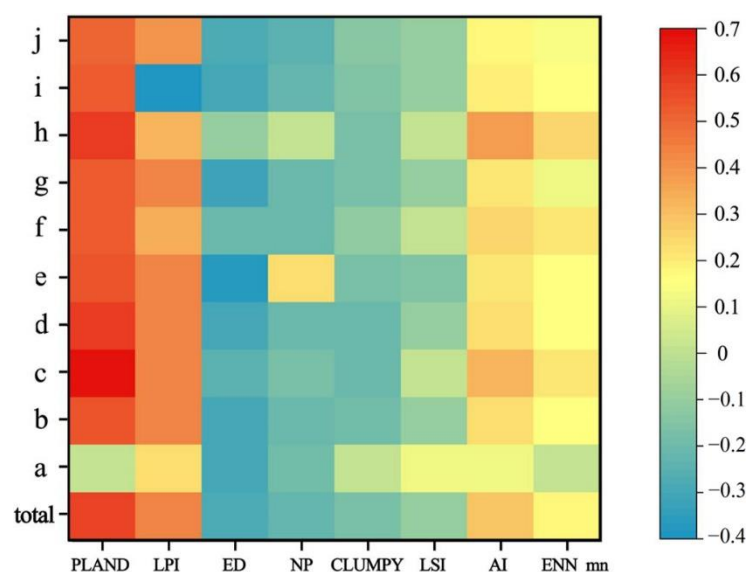
Figure 12. Correlation between landscape patterns index and ecosystem service value (ESV). Abbreviations: a (food production), b (material production), c (gas regulation), d (climate regulation), e (purified environment), f (hydrological regulation), g (soil conservation), h (main nutrient cycle), i (biodiversity), j (aesthetic landscape).

4. Discussion

4.1. Combination of LCS and PLUS Model

The changing landscape patterns of an area are dynamic in a nonlinear mode, involving complex layers of landscape change, and represent a typical complex system [42]. This complexity poses significant challenges for landscape planning and ecosystem management. To overcome these challenges, various simulation models have been developed to accurately, effectively, and dynamically inform regional landscape planning. The PLUS model used in this study had a high prediction accuracy for large regions, and its maximum Kappa coefficient for the simulation of future landscape types in the coastal region of Fujian was 0.889, higher than those of other models. Therefore, it is extremely credible that LCS was included in PLUS model as a constraint condition to forecast future landscape pattern changes [43]. Zhao et al. used the PLUS model to create three scenarios and successfully predicted the landscape structure of Wuhan in 2035. The simulation results were compared with those of other models, and the simulation accuracy was higher; therefore, the landscape pattern was most similar [44]. In conclusion, the simulation results of the PLUS model became more accurate and reliable in the various scenarios. The model was used in this study to simulate the landscape patterns of Fujian coastal areas, giving the alternative futures of a LCS and NDS in 2050. This provides substantial guidance and flexibility for decision-makers to manage landscape patterns under different development goals.

4.2. Interrelationship between Landscape Patterns and ESV

The evolution of the landscape at the surface causes changes in the regional landscape, area, and spatial location, with different landscape types providing different ecosystem services [45]. Comparing the landscape patterns and ESV changes in the study area, it was found that there was high consistency between the two. The accelerated urbanisation and industrialisation, and massive increase of population in Fujian coastal areas have direct impacts on landscape patterns, and consequently the entire ecosystem [46]. The rate of ESV loss was higher in areas with significant changes in the landscape patterns. Correlation-matrix analysis of the relationship between landscape type and ESV proved important and effective as a way of studying the spatial patterns [47].

We concluded that the changes in cultivated and construction lands in Fujian coastal areas exerted the greatest impact on the overall ESV. The major ways in which the cultivated

land increased ESV were through conversion to water and woodland, but its significant conversion to construction land eventually caused the ESV to fall. Since the expansion of construction land in Fujian coastal areas, in particular, in the Min Delta, has not yet ended, it is important to follow the land-use target of limiting the building area [48]. Similar to cultivated land, the extensive conversion of woodland to construction land significantly reduced the total ESV. As the ecosystem with the major productivity in the research region, forests made up approximately 55% of the total area, but provided approximately 74% of the ESV annually. Therefore, the forest protection red line should ensure that it is not subject to government intervention, and it is essential to monitor the spatiotemporal dynamics of the conversions from farmland to forests in the Fujian coastal areas [49]. The ESV simulated in 2050 in this study was higher under LCS than NDS. The results of the study are useful in providing guidance for the construction and development of the coastal areas in Fujian from the perspective of optimising the ESV.

The use of correlation analysis to quantify the association between the landscape pattern index and ESV was beneficial for developing a more reasonable ecosystem spatial pattern [50]. This study showed that the total ESV of the coastal Fujian was significantly positively correlated with PLAND, LPI and AI, and negatively correlated with ED and NP, indicating that the more complex the landscape shape was, the greater the number of landscapes, and the lower the ecological service value. This is consistent with the findings by Hou et al. for the city of Xi'an, in which the ESV was significantly positively correlated with FRAC_mn, PLAND, and AI, and strongly negatively correlated with ED and PD [51]. However, Lu et al. showed that the total ESV in Nanjing was positively correlated with LPI, negatively correlated with CONTAG, and not strongly correlated with PD, SHDI, or SPLIT [52]. This shows that there are differences between landscape patterns and ESV and their interrelationships in the study areas, and different landscape patterns have different ecological effects and affect ESs. Therefore, the relationship between landscape pattern changes and ESV is not simply non-causal, and the ecological and geographical significance of this relationship must be explored [53].

4.3. Policy Guidance

With the introduction of China's 'double carbon' target and carbon-peaking initiatives, enhancing ESV by gradually restoring the ecological environment and implementing greening initiatives is an important technical means to achieve the 'double carbon' target [54]. The basic direction of the relationship between the 'double carbon' target and ESV in the new development pattern is to combine policy orientation with technology integration to build rich and beautiful low-carbon cities. This study is based on a low carbon context, and through the establishment of the LCS scenario, the landscape structure is adjusted to ultimately achieve the ESV enhancement target for Fujian coastal areas. The results of the study show that the ESV value of the coastal region of Fujian in 2050 under the LCS scenario is 125.109 billion, which is 1.294 billion higher than that of the NDS. Therefore, the scenario setting established under the policy guidance is successful in optimising the landscape structure for this study, which can provide a theoretical basis for the low-carbon landscape-use pattern and ecological civilisation construction, and also provide the spatial basis for the future coordinated conservation and development of the coastal areas of Fujian [55].

4.4. Limitations of the Study and Future Work

Landscape pattern changes are a complex and dynamic process, and the analysis of historical data alone cannot fully predict changes in landscape patterns. By analysing landscape patterns in past and simulated scenarios, the impact of future landscape pattern changes on ESV under the influence of low-carbon targets was explored [56]. The results of this study enrich the research on the future ESV impacts of landscape pattern changes in coastal Fujian, and can also be used as a reference for landscape pattern changes and ESV studies in other larger regions. However, accurate assessment of ESV is a great challenge,

and the equivalence-factor method we used is an alternative method that can easily and quickly assess regional ESV levels [57]. The standard value of ESV, measured by the economic value of grain production per unit area, changes with the development of the market economy. The price change of crop varieties over time is not considered, making the ESV prediction inaccurate to some extent [58]. Increases or decreases in landscape area and changes in spatial layout can certainly lead to changes in the shape and connectivity of patches in the study area, which in turn affect the value of ecosystem services. However, changes in implicit patterns such as land quality, inputs, and outputs can also affect regional landscape patterns and ESV; therefore, changes in landscape patterns caused by socioeconomic factors and implicit land pattern shifts should be taken into account in the future [59]. Finally, because of the complexity of the social and natural composition of construction land, the ESV of construction land was ignored in the calculation process, and the estimation of the ESV of construction land needs to be addressed in future studies.

5. Conclusions

This study uses the PLUS model to simulate dynamic changes in landscape patterns and ESV in 2050 under the LCS. By exploring the correlation between different types of landscape areas, landscape pattern indices, and ESV, an attempt was made to find the intrinsic link between them, with the following conclusions:

1. The historical and simulated landscape types were similar in spatial distribution, and the woodland landscape type had the largest area, followed by cultivated land and grassland. The construction land in Quanzhou, Xiamen, and Zhangzhou accounted for 69% of the total construction land area, whereas Fuzhou accounted for 18%. From 2030 to 2050, the construction land area under LCS will account for 5.58%, 6.62% to 7.67%, whereas that under NDS will account for 7.65%, 8.57% to 9.45% of the total area.

2. At the landscape scale, the ED, LSI, PD, and IJI indices increased, the CONTAG and AREA_mn indices decreased, and the PAFRAC and SHAPE_mn indices did not fluctuate significantly. At the landscape type scale, woodland land was the dominant landscape in the study area, and its LPI and PLAND indices were always high. The two indices of construction land increased on a yearly basis, whereas the other landscape types decreased, and the declining trend of LCS was relatively slow. The PD, NP, and ED indices of each landscape type showed a rising trend, whereas the CLUMPY and AI indices decreased. The changes in these indices indicate that the landscape shape in the Fujian coastal areas tended to be complex and fragmented, the continuity of landscape types became low, and the aggregation of patches became weak.

3. The total value of ESV in coastal Fujian decreased by 3.134 billion from 2000 to 2020, and the LCS resulted in a 1.294 billion higher ESV in 2050 than the NDS, indicating that the optimised LUCC structure is consistent with low-carbon conservation objectives. Among the individual ESs, the contribution of regulating services is approximately 67%, and support services are more than 20%. Climate regulation, hydrological regulation, soil conservation, biodiversity, and gas regulation are the most important ecosystem service functions in coastal Fujian.

4. Over the past 20 years, the total ESV has decreased by 3.134 billion yuan. Except for the slightly higher ESV in the water area, the ESV of the other landscape types decreased. Urban expansion came at the cost of cultivated land loss, with a decline in ESV of 11.39% for cultivated land in the natural conservation scenario and 4.10% in the LCS. The total ESV values in the study area were significantly and positively correlated with cultivated land, woodland, and grassland and significantly and negatively correlated with construction land. The total ESV values were significantly and positively correlated with PLAND, LPI, and AI indices and significantly and negatively correlated with ED and NP, whereas the remaining correlations were not strong.

Appendix A

Table A1. Coefficients of ecosystem service value (ESV) per unit area in study area. (RMB/ha/year).

Data Type	Data	Year	Resolution	Source
Base Data	Land-use data	2000–2020	30 m	CAS (https://www.resdc.cn/, accessed on 28 November 2022)
Natural factors	DEM	2016	30 m	DEM generated by NASA SRTM1 v3.0
	Slope			Extracted from DEM
	Temperature	2019	1 km	CAS (https://www.resdc.cn/, accessed on 28 November 2022)
	Precipitation			
	Soil type	2008		
	Distance to water	2018	30 m	OpenStreetMap (https://www.openstreetmap.org/, accessed on 28 November 2022)
Socioeconomic factors	Population	2018	1 km	CAS (https://www.resdc.cn/, accessed on 28 November 2022)
	GDP			
	night-light		30 m	
Accessibility factors	Distance to trunk road		30 m	OpenStreetMap (https://www.openstreetmap.org/, accessed on 28 November 2022)
	Distance to primary road			
	Distance to secondary road			
	Distance to tertiary road			
	Distance to railway			
	Distance to railway station			
Constraint factors	Open water	2018	30 m	OpenStreetMap (https://www.openstreetmap.org/, accessed on 28 November 2022)

Table A2. Landscape type conversion-cost matrix under two scenarios.

2000–2020	LCS						NDS					
	a	**b**	**c**	**d**	**e**	**f**	**a**	**b**	**c**	**d**	**e**	**f**
a	1	0	0	0	0	0	1	0	1	0	0	0
b	0	1	1	0	0	0	0	1	1	0	1	1
c	0	1	1	0	0	0	1	1	1	1	1	1
d	0	0	0	1	0	0	0	1	1	1	1	1
e	1	1	1	0	1	0	1	1	1	0	1	1
f	1	1	1	0	1	1	1	1	1	0	1	1

a, b, c, d, e and f represent cultivated land, woodland land, grassland, water, construction land, and unused land, respectively; rows within the matrix indicate transfers out and columns indicate transfers in.

Table A3. Description of landscape pattern index.

Landscape Metrics	The Description of Metrics
$NP = n_i$	n_i = number of patches in the landscape patch type (class) i
$PD = \frac{n_i}{A}(100,000)(100)$	n_i = number of patches in the landscape patch type (class) i A = total landscape area (m^2). Units: per 100 ha
$Area\_mn = \frac{\sum_{i=1}^{m} x_i}{N}$	x_i = The area of patch I; N = The area of patchs
$PLAND = \frac{\sum_{j=1}^{n} a_{ij}}{A} \times 100$	a_{ij} = the area of a patch in a certain landscape type; A = the sum of the areas of all landscapes
$LPI = \frac{\max_{j=1}^{n}(a_{ij})}{A} \times 100$	a_{ij} = the area of patch IJ A = the total area of the landscape; including the internal background of the landscape
$Enn\_mn = cv(mean[patch_{ij}])$	$ENN[patch_{ij}]$ = the Euclidean nearest-neighbour distance of each patch.
$ED = \frac{E}{A} 10^6$	E = Total boundary length; A = Total boundary area
$LSI = \frac{e_i}{min e_i}$	e_i = total length of edge (or perimeter) by class i in terms of number of cell surfaces; includes all landscape boundary and background edge segments involving class I min_{ei} = minimum total length of edge (or perimeter) of class i in terms of number of cell surfaces. units:%
$CLUMPY = \left[\begin{array}{c} \frac{G_i - P_i}{P_i} \text{ for } G_i < P_i \& P_i < 0.5, \text{ else} \\ \frac{G_i - P_i}{1 - P_i} \end{array}\right]$	G_i = Similar to the adjacent; P_i = Focal patch type
$AI = \left[\frac{g_{ii}}{max \rightarrow g_{ii}}\right](100)$	g_{ii} = Number of similar adjacent patches of the corresponding landscape type
$CONTAG = \left[1 + \frac{\sum_{i=1}^{m}\sum_{k=1}^{m}\left[P_i\left\{\frac{g_{ik}}{\sum_{k=1}^{m} g_{ik}}\right\}\right]\cdot\left[\ln P_i\left\{\frac{g_{ik}}{\sum_{k=1}^{m} g_{ik}}\right\}\right]}{2\ln m}\right] \times 100$	P_i = proportional abundance of each patch type (i) g_{ik} = number of adjacencies (k) between cells of patch type (i) m = number of different patch types units: %
$IJI = \frac{-\sum_{i=1}^{m'}\sum_{k=i+1}^{m'}\left[\left(\frac{e_{ik}}{E}\right)*\ln\left(\frac{e_{ik}}{E}\right)\right]}{\ln\left(\frac{[m'(m'-1)]}{2}\right)}$	e_{ik} = the length (m) of each unique edge type E = the total landscape edge (m') = number of patch types

Table A4. Equivalent factors of ecosystem service value (ESV).

Ecosystem Service	Class	Cultivated Land	Woodland	Grassland	Water	Construction Land	Unused Land
Supply Service	FP	1.36	0.23	0.23	0.26	0	0.01
	MP	0.09	0.54	0.34	0.25	0	0.03
	GR	1.11	1.76	1.21	0.96	0	0.11
Regulation Service	CR	0.57	5.27	3.19	1.80	0	0.10
	PE	0.17	1.57	1.05	1.85	0	0.31
	HR	2.72	3.81	2.34	12.13	0	0.21
	SC	0.01	2.14	1.47	1.17	0	0.13
Support Service	MNC	0.19	0.16	0.11	0.09	0	0.01
	BD	0.21	1.95	1.34	3.95	0	0.12
Cultural Service	AL	0.09	0.86	0.59	2.37	0	0.05

Abbreviations: food production (FP), material production (MP), water resources supply (MRS), gas regulation (GR), climate regulation (CR), purified environment (PE), hydrological regulation (HR), soil conservation (SC), maintain nutrient cycle (MNC), biodiversity (BD), aesthetic landscape (AL).

Table A5. Landscape type transition matrix in coastal areas of Fujian from 2000 to 2020/km^2.

		2020						Transfer out
		Cultivated Land	Woodland	Grassland	Water	Construction Land	Unused Land	
2000	Cultivated land	10629	58	14	89	1361	0	1522
	Woodland	35	28645	136	47	520	1	739
	Grassland	12	362	8291	11	229	2	616
	Water	15	9	12	995	199	5	240
	Construction land	8	6	5	15	1704	0	34
	Unused land	0	0	2	0	1	38	3
	Transfer in	70	435	169	162	2319	8	
	Land area gain or loss	−1452	−304	−447	−78	2276	5	

References

1. Chen, Y.; Lu, H.; Li, J.; Xia, J. Effects of land use cover change on carbon emissions and ecosystem services in chengyu urban agglomeration, China. *Stoch. Environ. Res. Risk Assess.* **2020**, *34*, 1197–1215. [CrossRef]
2. Liu, X.; Li, S. A comparison analysis of the decoupling carbon emissions from economic growth in three industries of Heilongjiang province in China. *Environ. Sci. Pollut. Res.* **2021**, *28*, 65200–65215. [CrossRef] [PubMed]
3. Gao, S.; Zhang, H. Urban planning for low-carbon sustainable development. *Sustain. Comput. Inform. Syst.* **2020**, *28*, 100398. [CrossRef]
4. Cheng, R.; Wang, F. Land Use Benefit Evaluation and Barrier Diagnosis of Pearl River Delta from the Perspective of Low-Carbon Ecological City. Res. *Soil Water Conserv.* **2021**, *28*, 351–359.
5. Zhang, Z.P.; Xia, F.Q.; Yang, D.G.; Huo, J.W.; Wang, G.L.; Chen, H.X. Spatiotemporal characteristics in ecosystem service value and its interaction with human activities in Xinjiang, China. *Ecol. Indic.* **2020**, *110*, 105826. [CrossRef]
6. Wang, X.; Pan, T.; Pan, R.; Chi, W.; Ma, C.; Ning, L.; Wang, X.; Zhang, J. Impact of Land Transition on Landscape and ecosystem service value in Northeast Region of China from 2000–2020. *Land* **2022**, *11*, 696. [CrossRef]
7. Chamling, M.; Bera, B. Spatio-temporal Patterns of Land Use/Land Cover Change in the Bhutan–Bengal Foothill Region Between 1987 and 2019. Study Towards Geospatial Applications and Policy Making. *Earth Syst. Eviron.* **2020**, *4*, 117–130. [CrossRef]
8. Costanza, R.; d'Arge, R.; de Groot, R.; Farber, S.; Grasso, M.; Hannon, B.; Limburg, K.; Naeem, S.; O'Neill, R.V.; Paruelo, J. The value of the world's ecosystem services and natural capital. *Nature* **1997**, *387*, 53–260. [CrossRef]
9. Xie, L.; Wang, H.; Liu, S. The ecosystem service value simulation and driving force analysis based on land use/land cover: A case study in inland rivers in arid areas of the Aksu River Basin, China. *Ecol. Indic.* **2022**, *38*, 108828. [CrossRef]
10. Gao, X.; Wang, J.; Li, C.; Shen, W.; Song, Z.; Nie, C.; Zhang, X. Land use change simulation and spatial analysis of ESV in Shijiazhuang under multi-scenarios. *Environ. Sci. Pollut. Res.* **2021**, *28*, 31043–31058. [CrossRef]
11. Su, K.; Wei, D.Z.; Lin, W.X. Evaluation of ecosystem services value and its implications for policy making in China: A case study of Fujian province. *Ecol. Indic.* **2020**, *108*, 105752. [CrossRef]
12. Zhang, J.; Qu, M.; Wang, C.; Zhao, J.; Cao, Y. Quantifying landscape pattern and ecosystem service value changes: A case study at the county level in the Chinese Loess Plateau. *Glob. Ecol. Conserv.* **2020**, *23*, e01110. [CrossRef]
13. Jiang, W.; Lu, Y.; Liu, Y.; Gao, W. ESV of the Qinghai-Tibet Plateau significantly increased during 25 years. *Ecosyst. Serv.* **2020**, *44*, 101146. [CrossRef]
14. Pan, N.; Guan, Q.; Wang, Q.; Sun, Y.; Li, H.; Ma, Y. Spatial Differentiation and Driving Mechanisms in ecosystem service value of Arid Region: A case study in the middle and lower reaches of Shule River Basin, NW China. *J. Clean. Prod.* **2021**, *319*, 128718. [CrossRef]
15. Yang, X.; Chen, R.; Zheng, X.Q. Simulating land use change by integrating ANN-CA model and landscape pattern indices. *Geomat. Nat. Hazards Risk* **2016**, *7*, 918–932. [CrossRef]
16. Chen, Y.; Li, X.; Liu, X.; Ai, B. Modeling urban land-use dynamics in a fast developing city using the modified logistic cellular automaton with a patch-based simulation strategy. *J. Geogr. Sci.* **2014**, *28*, 234–255. [CrossRef]
17. Liu, X.; Liang, X.; Li, X.; Xu, X.; Ou, J.; Chen, Y.; Li, S.; Wang, S.; Pei, F. A future land use simulation model (FLUS) for simulating multiple land use scenarios by coupling human and natural effects. *Landsc. Urban. Plan.* **2017**, *168*, 94–116. [CrossRef]
18. Liang, X.; Guan, Q.; Clarke, K.C.; Liu, S.; Wang, B.; Yao, Y. Understanding the drivers of sustainable land expansion using a patch-generating land use simulation (PLUS) model: A case study in Wuhan, China. *Comput. Environ. Urban. Syst.* **2021**, *85*, 101569. [CrossRef]
19. Wang, B.; Liao, J.; Zhu, W.; Qiu, Q.; Tang, L. The weight of neighborhood setting of the FLUS model based on a historical scenario: A case study of land use simulation of urban agglomeration of the Golden Triangle of Southern Fujian in 2030. *Acta Ecol. Sin.* **2019**, *39*, 4284–4298.
20. Lin, L.; Qiu, H. The Changes and Driving Factors of Coastal Areas Land Use in Time and Space: A Case Study in Fujian Province, Southeast China. *Pol. J. Environ. Stud.* **2022**, *31*, 2695–2707. [CrossRef]

21. Li, S.; Cao, Y.; Liu, J.; Wang, S.; Zhou, W. Assessing Spatiotemporal Dynamics of Land Use and Cover Change and Carbon Storage in China's Ecological Conservation Pilot Zone: A Case Study in Fujian Province. *Remote Sens.* **2022**, *14*, 4111. [CrossRef]

22. Zhang, X.; Du, H.; Wan, Y.; Chen, Y.; Ma, L.; Dong, T. Watershed landscape ecological risk assessment and landscape pattern optimization: Take Fujiang River Basin as an example. *Hum. Ecol. Risk Assess.* **2021**, *27*, 2254–2276. [CrossRef]

23. Chen, X.; He, X.; Wang, S. Simulated Validation and Prediction of Land Use under Multiple Scenarios in Daxing District, Beijing, China, Based on GeoSOS-FLUS Model. *Sustainability* **2022**, *14*, 11428. [CrossRef]

24. Shi, M.; Wu, H.; Fan, X.; Jia, H.; Dong, T.; He, P.; Baqa, M.; Jiang, P. Trade-Offs and Synergies of Multiple Ecosystem Services for Different Land Use Scenarios in the Yili River Valley, China. *Sustainability* **2021**, *13*, 1577. [CrossRef]

25. Pontius, R.G.; Boersma, W.; Castella, J.C.; Clarke, K.; de Nijs, T.; Dietzel, C.; Duan, Z.; Fotsing, E.; Goldstein, N.; Kok, K. Comparing the input, output, and validation maps for several models of land change. *Ann. Reg. Sci.* **2008**, *42*, 11–37. [CrossRef]

26. Li, D.; Fan, K.; Lu, J.; Wu, S.; Xie, X. Research on Spatio-Temporal Pattern Evolution and the Coupling Coordination Relationship of Land-Use Benefit from a Low-Carbon Perspective: A Case Study of Fujian Province. *Land* **2022**, *11*, 1498. [CrossRef]

27. Zhao, J.S.; Yuan, L.; Zhang, M. A study of the system dynamics coupling model of the driving factors for multi-scale land use change. *Environ. Earth Sci.* **2016**, *75*, 529. [CrossRef]

28. Lu, C.; Qi, X.; Zheng, Z.; Jia, K. PLUS-model based multi-scenario land space simulation of the Lower Yellow River Region and its ecological effects. *Sustainability* **2022**, *14*, 6942. [CrossRef]

29. Jia, Y.; Tang, L.; Xu, M.; Yang, X. Landscape pattern indices for evaluating urban spatial morphology—A case study of Chinese cities. *Ecol. Indic.* **2019**, *99*, 27–37. [CrossRef]

30. Clement, F.; Ruiz, J.; Rodriguez, M.A.; Blais, D.; Campeau, S. Landscape diversity and forest edge density regulate stream water quality in agricultural catchments. *Ecol. Indic.* **2017**, *72*, 627–639. [CrossRef]

31. Zhao, Q.; Wen, Z.; Chen, S.; Ding, S.; Zhang, M. Quantifying land Use/land cover and landscape pattern changes and impacts on ecosystem services. *Int. J. Environ. Res. Public Health* **2019**, *17*, 126. [CrossRef] [PubMed]

32. Wu, M.; Li, C.; Du, J.; He, P.; Zhong, S.; Wu, P.; Lu, H.; Fang, S. Quantifying the dynamics and driving forces of the coastal wetland landscape of the Yangtze river estuary since the 1960s. *Reg. Stud. Mar. Sci.* **2019**, *32*, 100854. [CrossRef]

33. Ma, C.; Ai, B.; Zhao, J.; Xu, X.; Huang, W. Change detection of mangrove forests in coastal Guangdong during the past three decades based on remote sensing data. *Remote Sens.* **2019**, *11*, 921. [CrossRef]

34. Santos-Martin, F.; Zorrilla-Miras, P.; Palomo, I.; Montes, C.; Benayas, J.; Maes, J. Protecting nature is necessary but not sufficient for conserving ecosystem services: A comprehensive assessment along a gradient of land-use intensity in Spain. *Ecosyst. Serv.* **2019**, *35*, 43–51. [CrossRef]

35. Xie, G.; Zhang, C.; Zhen, L.; Zhang, L. Dynamic changes in the value of China's ecosystem services. *Ecosyst. Serv.* **2017**, *26*, 146–154. [CrossRef]

36. Xiao, H.; Hu, C.; Chi, Y. Preliminary evaluation of ecosystem service value of natural grassland in China. *Fresen. Environ. Bull.* **2021**, *30*, 2670–2685.

37. Estoque, R.C.; Murayama, Y. Quantifying landscape pattern and ecosystem service value changes in four rapidly urbanizing hill stations of Southeast Asia. *Landsc. Ecol.* **2016**, *31*, 1481–1507. [CrossRef]

38. Brozovic, D.; Tregua, M. The evolution of service systems to service ecosystems: A literature review. *Int. J. Manag. Rev.* **2022**, *24*, 459–479. [CrossRef]

39. Yun, J.; Liu, H.M.; Xu, Z.C.; Cao, X.A.; Ma, L.Q.; Wen, L.; Zhuo, Y.; Wang, L.X. Assessing changes in the landscape pattern of wetlands and its impact on the value of wetland ecosystem services in the Yellow River Basin, Inner Mongolia. *Sustainability* **2022**, *14*, 6328. [CrossRef]

40. Solomon, N.; Segnon, A.C.; Birhane, E. Ecosystem service value changes in response to land-use/land-cover dynamics in dry afromontane forest in Northern Ethiopia. *Int. J. Environ. Res. Public Health* **2019**, *16*, 4653. [CrossRef]

41. Wang, D.; He, W.; Shi, R. How to achieve the dual-control targets of China's CO_2 emission reduction in 2030? Future trends and prospective decomposition. *J. Clean. Prod.* **2019**, *213*, 1251–1263. [CrossRef]

42. Fang, Z.; Ding, T.; Chen, J.; Xue, S.; Zhou, Q.; Wang, Y.; Wang, Y.; Huang, Z.; Yang, S. Impacts of land use/land cover changes on ecosystem services in ecologically fragile regions. *Sci. Total Environ.* **2022**, *831*, 154967. [CrossRef] [PubMed]

43. Xiao, Y.; Huang, M.; Xie, G.; Zhen, L. Evaluating the impacts of land use change on ecosystem service value under multiple scenarios in the Hunshandake region of China. *Sci. Total Environ.* **2022**, *850*, 158067. [CrossRef] [PubMed]

44. Lou, Y.; Yang, D.; Zhang, P.; Zhang, Y.; Song, M.; Huang, Y.; Jing, W. Multi-scenario simulation of land use changes with ecosystem services value in the Yellow River Basin. *Land* **2022**, *11*, 992. [CrossRef]

45. Zhai, H.; Lv, C.; Liu, W.; Yang, C.; Fan, D.; Wang, Z.; Guan, Q. Understanding spatio-temporal patterns of land use/land cover change under urbanization in Wuhan, China, 2000–2019. *Remote Sens.* **2021**, *13*, 3331. [CrossRef]

46. Zhang, L.; Jin, G.; Wan, Q.; Liu, Y.F.; Wei, X.J. Measurement of ecological land use/cover change and its varying spatiotemporal driving forces by statistical and survival analysis: A case study of Yingkou City, China. *Sustainability* **2018**, *10*, 4567. [CrossRef]

47. Zang, Z.; Zou, X.; Zuo, P.; Song, Q.; Wang, C.; Wang, J. Impact of landscape patterns on ecological vulnerability and ecosystem service values: An empirical analysis of Yancheng Nature Reserve in China. *Ecol. Indic.* **2017**, *72*, 142–152. [CrossRef]

48. Jia, Y.; Tang, X.; Liu, W. Spatial–temporal evolution and correlation analysis of ecosystem service value and landscape ecological Risk in Wuhu City. *Sustainability* **2020**, *12*, 2803. [CrossRef]

49. Zhang, S.; Zhong, Q.; Cheng, D. Coupling coordination analysis and prediction of landscape ecological risks and ecosystem services in the Min River Basin. *Land* **2022**, *11*, 222. [CrossRef]

50. Guo, P.; Zhang, F.; Wang, H. The response of ecosystem service value to land use change in the middle and lower Yellow River: A case study of the Henan section. *Ecol. Indic.* **2022**, *140*, 109019. [CrossRef]

51. Luo, C.; Fu, X.; Zeng, X.; Cao, H.; Wang, J. Responses of remnant wetlands in the Sanjiang Plain to farming-landscape patterns. *Ecol. Indic.* **2022**, *135*, 108542. [CrossRef]

52. Hou, L.; Wu, F.; Xie, X. The spatial characteristics and relationships between landscape pattern and ecosystem service value along an urban-rural gradient in Xi'an city, China. *Ecol. Indic.* **2020**, *108*, 105720. [CrossRef]

53. Lu, M.; Zhang, Y.; Liang, F.; Wu, Y. Spatial relationship between land use patterns and ecosystem services value—Case study of Nanjing. *Land* **2022**, *11*, 1168. [CrossRef]

54. Hasan, S.; Zhen, L.; Miah, M.G.; Ahamed, T.; Samie, A. Impact of land use change on ecosystem services: A review. *Environ. Dev.* **2020**, *34*, 100527. [CrossRef]

55. Wang, Y.; Zhang, S.; Zhen, H.; Chang, X.E.; Shataer, R.; Li, Z. Spatiotemporal evolution characteristics in ecosystem services value based on land use/cover change in the Tarim River Basin, China. *Sustainability* **2020**, *12*, 7759. [CrossRef]

56. Liao, J.; Peng, X.; Wang, Q.; Jian, P.; Wu, Q. Study on the coupling and coordination relationship of urban land use benefit in urban agglomeration on the west coast of Taiwan Strait. *World Reg. Stud.* **2021**, *30*, 556–566.

57. Aksoy, H.; Kaptan, S. Simulation of future forest and land use/cover changes (2019–2039) using the cellular automata-Markov model. *Geocarto Int.* **2022**, *37*, 1183–1202. [CrossRef]

58. Qiu, J.; Huang, T.; Yu, D. Evaluation and optimization of ecosystem services under different land use scenarios in a semiarid landscape mosaic. *Ecol. Indic.* **2022**, *135*, 108516. [CrossRef]

59. Li, Y.; Zhan, J.; Liu, Y.; Zhang, F.; Zhang, M. Response of ecosystem services to land use and cover change: A case study in Chengdu City. *Resour. Conserv. Recycl.* **2018**, *132*, 291–300. [CrossRef]